Regulation of intestinal Cl^- and HCO_3^- secretion by uroguanylin

NAM SOO JOO,[1] ROSLYN M. LONDON,[1,2] HYUN DJU KIM,[1]
LEONARD R. FORTE,[1,2] AND LANE L. CLARKE[3,4]
[1]*Department of Pharmacology, School of Medicine,* [3]*Department of Veterinary Biomedical Sciences, College of Veterinary Medicine, and the* [4]*Dalton Cardiovascular Research Center, University of Missouri and* [2]*The Truman Veterans Affairs Medical Center, Columbia, Missouri 65212*

Joo, Nam Soo, Roslyn M. London, Hyun Dju Kim, Leonard R. Forte, and Lane L. Clarke. Regulation of intestinal Cl^- and HCO_3^- secretion by uroguanylin. *Am. J. Physiol.* 274 (*Gastrointest. Liver Physiol.* 37): G633–G644, 1998.—Uroguanylin is an intestinal peptide hormone that may regulate epithelial ion transport by activating a receptor guanylyl cyclase on the luminal surface of the intestine. In this study, we examined the action of uroguanylin on anion transport in different segments of freshly excised mouse intestine, using voltage-clamped Ussing chambers. Uroguanylin induced larger increases in short-circuit current (I_{sc}) in proximal duodenum and cecum compared with jejunum, ileum, and distal colon. The acidification of the lumen of the proximal duodenum (pH 5.0–5.5) enhanced the stimulatory action of uroguanylin. In physiological Ringer solution, a significant fraction of the I_{sc} stimulated by uroguanylin was insensitive to bumetanide and dependent on HCO_3^- in the bathing medium. Experiments using pH-stat titration revealed that uroguanylin stimulates serosal-to-luminal HCO_3^- secretion ($J_{s\rightarrow l}^{HCO_3^-}$) together with a larger increase in I_{sc}. Both $J_{s\rightarrow l}^{HCO_3^-}$ and I_{sc} were significantly augmented when luminal pH was reduced to pH 5.15. Uroguanylin also stimulated the $J_{s\rightarrow l}^{HCO_3^-}$ and I_{sc} across the cecum, but luminal acidity caused a generalized decrease in the bioelectric responsiveness to agonist stimulation. In cystic fibrosis transmembrane conductance regulator (CFTR) knockout mice, the duodenal I_{sc} response to uroguanylin was markedly reduced, but not eliminated, despite having a similar density of functional receptors. It was concluded that uroguanylin is most effective in acidic regions of the small intestine, where it stimulates both HCO_3^- and Cl^- secretion primarily via a CFTR-dependent mechanism.

cyclic GMP; bicarbonate transport; chloride transport; cystic fibrosis; cystic fibrosis transmembrane conductance regulator; guanylyl cyclase; mouse intestine; proximal duodenum

UROGUANYLIN is an intestinal peptide that is closely related to guanylin, another intestinal peptide that is secreted onto the intestinal epithelial surface and regulates transepithelial salt and water transport through a receptor-mediated action (19, 26, 27, 34, 50). Guanylin was first discovered in attempts to identify an endogenous ligand for the apical membrane-bound guanylyl cyclase C, which serves as the receptor for *Escherichia coli* heat-stable enterotoxin (STa) (6, 13, 20, 35, 36, 48, 54, 55), the causative agent of traveler's diarrhea (12). Guanylin binding to the receptor increases intracellular cGMP, resulting in activation of protein kinase G II in the intestinal epithelial cell (18, 45). The subsequent intracellular events include stimulation of anion secretion via the cystic fibrosis transmembrane conductance regulator (CFTR) (3, 7, 16, 21) and possibly the inhibition of electroneutral NaCl absorption (37, 52). Much less is known about the intestinal actions of uroguanylin. However, it has been shown that the peptide stimulates intracellular cGMP production and transepithelial Cl^- secretion in T84 cells, a cell line derived from a colonic adenocarcinoma (17, 24, 27). Both uroguanylin and guanylin are abundantly expressed in the intestinal epithelium as inactive precursors, or propeptides, that undergo enzymatic cleavage to yield the bioactive peptides (11, 29, 43). Uroguanylin and, to a lesser extent, guanylin are expressed in other tissues and have been isolated from plasma and urine (11, 25, 27, 28, 40, 44, 46). Recent studies demonstrate that uroguanylin induces natriuresis in the perfused rat kidney (M. Fonteles, personal communication), suggesting that (intestinal) uroguanylin may also be elaborated into the blood as an endocrine mediator of renal function (14).

Although uroguanylin and guanylin share nearly 50% identity in their primary amino acid sequences, uroguanylin differs from guanylin with regard to intestinal expression and intrinsic biochemical properties (26, 27, 34). First, both uroguanylin and guanylin are found throughout the length of the rat intestinal mucosa, but uroguanylin mRNA is most abundant in the proximal small intestine, whereas guanylin mRNA is greatest in the distal small intestine and large bowel (39, 40, 42). In opossums, uroguanylin mRNA is abundant in the duodenum but also has high levels of expression in the large intestine compared with guanylin (11). Second, the amino acid sequence of uroguanylin has a conserved asparagine residue, instead of the phenylalanine (in opossum) or tyrosine (in other species) found in guanylin, which makes uroguanylin resistant to proteolysis by the pancreatic enzyme chymotrypsin (25). Third, uroguanylin has two additional acidic amino acids that render it a more strongly acidic molecule. Interestingly, uroguanylin is more potent at acidic pH, whereas guanylin is more potent at alkaline pH, in stimulating cGMP production and Cl^- secretion in T84 cell monolayers (24, 27).

The effects of uroguanylin on anion secretion have not been previously examined in the intact mammalian intestinal mucosa. On the basis of its higher expression in duodenum and its pH dependence of action, it was reasoned that uroguanylin may be more effective in regions of the intestinal tract where the mucosa is exposed to acidic luminal conditions. Therefore, different segments of the murine intestine were investigated for responsiveness to uroguanylin by measuring the

short-circuit current (I_{sc}), an index of anion secretion. In the most responsive intestinal segments (proximal duodenum and cecum), we examined the pH dependence of uroguanylin in stimulating transepithelial secretion of Cl^- and HCO_3^- across the mucosa.

MATERIALS AND METHODS

Animals

Female C57BL6 mice 8–10 wk old were housed in a standard animal care room with a 12:12-h light-dark cycle. Animals were allowed free access to food and water until the time of study. CFTR knockout and normal littermate mice (B6.129-*Cftr*$^{tm/UNC}$; C57BL/6J-*Cftr*$^{tm/UNC}$) were also maintained on standard laboratory chow, but the water contained an osmotic laxative (polyethylene glycol) to reduce intestinal malfunction in the *cftr(−/−)* mice (5). All experiments involving the animals were approved by the University Institutional Animal Care and Use Committee.

Tissue Preparation

Before each experiment, the mice were fasted for a minimum of 1 h and only water was provided. The mice were killed by a brief exposure to a 100% CO_2 gas atmosphere (to induce narcosis), followed immediately by a surgical pneumothorax. A midline abdominal incision was used to excise the gallbladder and the following intestinal segments: proximal duodenum (a portion from 2 mm distal to the pylorus to the sphincter of Oddi), midjejunum, ileum, cecum (a portion 1–2 cm proximal to the cecal apex), and distal colon. The excised segments were opened along the mesenteric border in ice-cold, oxygenated Krebs-Ringer-bicarbonate (KRB) solution and pinned mucosal-side down on a pliable silicone surface. The intestinal sections were stripped of their outer muscle layers by shallow dissection with a scalpel and fine forceps.

Bioelectric Measurements

Each intestinal sheet (~1 cm in length) and the microdissected gallbladder (with a support of nylon gauze) were mounted in standard Ussing chambers with an exposed surface area of 0.25 cm^2 for intestinal preparations (or 0.126 cm^2 for ileum and colon) and 0.049 cm^2 for the gallbladder as previously described (5). The tissue sheets were independently bathed on the serosal and mucosal surfaces with 4 ml of KRB solution containing (in mM) 115 NaCl, 4 K_2HPO_4, 0.4 KH_2PO_4, 25 $NaHCO_3$, 1.2 $MgCl_2$, and 1.2 $CaCl_2$, pH 7.4. To facilitate pH adjustment of the medium in some experiments, a phosphate-free Ringer solution of the following composition was used (in mM): 115 NaCl, 5 KCl, 25 $NaHCO_3$, 1.2 $MgSO_4$, and 1.2 calcium gluconate, pH 7.4. In ion substitution experiments, HCO_3^- and Cl^- were replaced with TES and gluconate, respectively. Glucose (10 mM) was included in the serosal solution (both baths in large intestinal preparations), and 10 mM mannitol was substituted for glucose in the mucosal bath to prevent Na^+-coupled glucose current stimulation. To minimize tissue exposure to endogenously generated prostaglandins during tissue preparation and mounting, indomethacin (1.0 μM) was present in both baths throughout the experiment. KRB solutions were gassed with 95% O_2-5% CO_2, whereas HCO_3^--free bathing solutions were gassed with 100% O_2. The solutions were circulated via a gas-lift recirculation system and were maintained at 37°C by water-jacketed reservoirs. In all experiments, TTX (0.1 μM) was added to the serosal bath at least 20 min before each experiment to prevent any intrinsic neural influence on ion transport regulation of the intestine (47).

Transmural I_{sc} (μA/cm^2 tissue surface area) was measured with the use of an automatic voltage clamp device (VCC-600; Physiologic Instruments, San Diego, CA) that compensates for electrode offset and the fluid resistance between the potential-measuring electrode bridges. Transepithelial potential difference (in mV) was measured via a pair of calomel half-cells connected to the serosal and mucosal baths by 4% agar-Ringer (wt/vol) bridges. I_{sc} was applied across the tissue via a pair of Ag/AgCl electrodes that were kept in contact with the serosal and mucosal baths through 4% agar-Ringer bridges. All experiments were carried out under short-circuited conditions. Total tissue conductance (G_t, mS/cm^2 tissue surface area) was calculated by applying Ohm's law to the current deflection resulting from a 5-mV bipolar pulse across the tissue every 5 min during the course of the experiment. In all cases, the serosal side served as ground and the I_{sc} was conventionally referred to as negative when current flowed from the lumen to the serosa.

After the tissues achieved a stable I_{sc} (~20 min post-TTX), a 20-min period was required to adjust the luminal bath pH. The small intestine and gallbladder preparations were then sequentially exposed to a peptide (uroguanylin, 1.0 μM; guanylin, 1.0 μM; or STa, 0.02 μM) in the luminal bath for 30 min and then to bumetanide (0.1 mM) in the serosal bath for 10 min to inhibit the Na^+-K^+-2 Cl^- cotransporter. After pH adjustment, large intestinal preparations were first treated with amiloride (0.1 mM) in the luminal bath for 20 min to inhibit electrogenic Na^+ absorption and were then treated with peptide addition followed by bumetanide. In studies in which the effects of acidic pH on the action of the peptides were examined, the proximal duodenum, jejunum, and cecum were used, and the pH of the luminal bath was decreased to pH 5.0–5.5 by addition of 1 N HCl. An equal amount of 1 M NaCl was added simultaneously to the serosal bath to prevent a transepithelial Cl^- diffusion potential. At the end of an experiment, glucose (10 mM) was added to the luminal bath of the small intestinal preparations and carbachol (CCh; 0.1 mM) was added to the serosal bath of the large intestinal preparations as measures of tissue viability.

Bioassay for cGMP Accumulation in Mouse Intestine

Mucosal epithelium was prepared by scraping the intestinal segment from *cftr(−/−)* and *cftr(+/+)* mice and washing it gently once in 0.9% NaCl and twice in DMEM containing 20 mM HEPES, pH 7.4. The mucosal suspension (~60 mg wet wt) was placed in 0.2 ml DMEM (pH 7.4) at 4°C. The tissue was incubated for 40 min at 37°C with either 1.0 μM uroguanylin, 1.0 μM guanylin, or vehicle that was added to the DMEM-HEPES with 1.0 mM 3-isobutyl-1-methylxanthine. At the end of the 40-min period, perchloric acid was added to a final concentration of 3.3%, the cells were centrifuged, and the resulting supernatants were neutralized with 1 N KOH. The supernatants were used to measure cGMP concentration by radioimmunoassay as described previously (15).

pH-Stat Titration

Proximal duodenum or cecum was mounted in a standard Ussing chamber bathed with 156.2 mM NaCl in the luminal bath and KRB in the serosal bath. In cecal experiments, 1.2 mM $CaCl_2$ and $MgCl_2$ were also added to the luminal bath. The luminal bath was gassed with 100% O_2 and the serosal bath with 95% O_2-5% CO_2. To decrease the pH of the luminal bath, the luminal saline solution was gassed with 95% O_2-5% CO_2 and maintained at pH 5.15. The serosal-to-luminal flux of HCO_3^- ($J_{s\to l}^{HCO_3^-}$) was measured by continuously titrat-

ing the luminal solution to pH 7.4 (or pH 5.15) with 5 mM HCl, using either a computer-aided titrimeter (model 455/465; Fisher) or manual addition of titrant. The volume of added acid was used to calculate the HCO_3^- flux, taking into account the exposed surface area of tissue (0.25 cm^2) and time. Typically, $J_{s\rightarrow l}^{HCO_3^-}$ stabilized within 30 min after the tissue was mounted and a basal flux period was initiated. After 30 min, uroguanylin (1.0 μM) was added to the luminal bath, and when the $J_{s\rightarrow l}^{HCO_3^-}$ stabilized (~20 min), a second 30-min flux period was initiated.

Receptor Autoradiography

Dissected intestinal segments (proximal duodenum, midjejunum, ileum, cecum, and distal colon) from control and CFTR knockout mice were quickly frozen with dry ice and stored at −80°C. The frozen tissue samples were sectioned to a 12-μm thickness in a cryostat device (2800 Frigocut N, Reichert-Jung; Leica Instrument, Germany) maintained at −20°C. Two sections were placed on opposite ends of a gelatin-coated slide, one for total binding (TB) and one for nonspecific binding (NSB), and then dried and stored at −80°C until used. Iodinated STa was used as the radioligand for this assay and was prepared by a modification of the method described by Krause and co-workers (35). The use of STa was necessary because iodination of guanylin (Tyr-9) may decrease the biological activity of this ligand (35) and uroguanylin has no tyrosine residue available for labeling. For the assay, each section on the slide was incubated with 30 μl of DMEM containing 0.5% BSA to minimize background labeling (pH 5.5 at 37°C for 20 min). Total binding of ^{125}I-labeled STa was assessed by incubating 30 μl DMEM containing 1,000 cpm/μl ^{125}I-STa on one section, and nonspecific binding was assessed by incubating 30 μl DMEM containing both ^{125}I-STa and unlabeled STa (1.0 μM), uroguanylin (10 μM), or guanylin (10 μM) on the other section. After a 20-min incubation at 37°C, slides were washed five times with ice-cold phosphate-buffered saline solution and then air-dried. To verify labeling in the different intestinal segments, the slides were arranged in cassettes and exposed to Kodak X-OMAT AR (XAR 5) film overnight at −80°C, and then the film was developed. Slides were then transferred in a dark room, coated with Kodak NTB-2 emulsion solution, and dried overnight. The emulsion-coated slides were sealed in light-tight boxes and stored at 4°C for 2–3 wk until they were developed. After development, fixation, and coverslipping, the radiolabeled TB and NSB sections were examined under bright- and dark-field microscopy.

Materials

Opossum uroguanylin (QEDCELCINVACTGC) and *E. coli* ST (CCELCCNPACTGC), STa13, were synthesized by the solid-phase method, using an Applied Biosystems peptide synthesizer, as previously described (25). Opossum uroguanylin differs from murine uroguanylin (TDECELCINVACTGC) only in the sequence of the first three amino acids. Purified rat guanylin (PNTCEICAYAACTGC) was generously provided by Dr. Mark Currie (Searle Research and Development, St. Louis, MO). The iodination of *E. coli* ST (NSSNYCCELCCNPACTGCY) was performed using a lactoperoxidase method as previously described (15, 16). Membrane-permeable 8-bromo-cAMP (8-BrcAMP) and 8-bromo-cGMP (8-BrcGMP) were obtained from Research Biochemical International (Natick, MA). All other chemicals were purchased from either Sigma Chemical (St. Louis, MO) or Fisher Scientific (Springfield, IL). Uroguanylin, guanylin, and *E. coli* STa were dissolved in deionized water at a stock concentration (s.c.) of 1 mM. TTX was dissolved in 0.2% acetic acid at a stock concentration of 0.1 mM. Indomethacin (s.c., 10 mM), bumetanide (s.c., 0.1 M), methazolamide (s.c., 1.0 M), DIDS (s.c., 0.3 M), and amiloride (s.c., 0.1 M) were dissolved in DMSO.

Data Analysis

Data are means ± SE. Student's *t*-test for paired or unpaired data or an ANOVA protected least-significant different test was used for comparisons of means among different intestinal segments and different treatment groups. In all cases, $P < 0.05$ was accepted as a statistically significant difference.

RESULTS

Segmental Responses to Uroguanylin in the Mouse Intestine

Figure 1*A* shows the pattern of I_{sc} responses to sequential treatment with specific agents on proximal duodenum. After the tissue was mounted, the addition of TTX (0.1 μM, serosal bath) resulted in a decrease in the baseline I_{sc} to a stable value within 20 min. Uroguanylin (1.0 μM, luminal bath) caused a rapid increase in I_{sc}, which was sustained for a 40-min period. Subsequent addition of STa (1.0 μM, luminal bath) elicited a further increase in I_{sc}. Bumetanide (0.1 mM, serosal bath) treatment resulted in a decrease in the I_{sc} but to a level that was elevated relative to the I_{sc} before the uroguanylin/STa treatment. The inhibitory effect of bumetanide on I_{sc} typically reached steady state by 10 min posttreatment, i.e., the percentage of bumetanide inhibition at 5 min was equal to 98 ± 1.1% of the I_{sc} at 10 min postbumetanide (n = 15) in proximal duodenum. Glucose (10 mM, luminal bath) addition intended to stimulate Na^+-coupled glucose transport caused a rapid increase in I_{sc}. In contrast to apical treatment, the addition of either uroguanylin or STa to the serosal bath solution had no effect on the I_{sc} (Fig. 1*B*).

Cumulative data of the I_{sc} responses to uroguanylin (1.0 μM) by different intestinal segments and the gallbladder are shown in Fig. 2. Uroguanylin elicited an I_{sc} response in all intestinal segments but had no stimulatory effect on the gallbladder preparations. Proximal duodenum and cecum had the greatest mean I_{sc} responses to uroguanylin (1.0 μM) and were not significantly different from each other. However, the I_{sc} response in the proximal duodenum was significantly greater than the responses in the other small intestinal segments (jejunum and ileum). Likewise, the cecum had a greater I_{sc} response than did the distal colon. The concentration of uroguanylin (1.0 μM) used in these experiments was not a maximally stimulatory dose, since subsequent addition of STa (1.0 μM) elicited further increases in the I_{sc} in all intestinal segments that were tested (ΔI_{sc}, in μA/cm^2): 95.5 ± 10.3 in proximal duodenum (n = 7), 112.0 ± 18.5 in jejunum (n = 9), 64.5 ± 10.5 in ileum (n = 9), 77.5 ± 15.8 in cecum (n = 9), and 58.4 ± 13.5 in distal colon (n = 7).

Proximal Duodenum

Effect of luminal acidic pH on uroguanylin action. To examine the effect of luminal acidity on uroguanylin

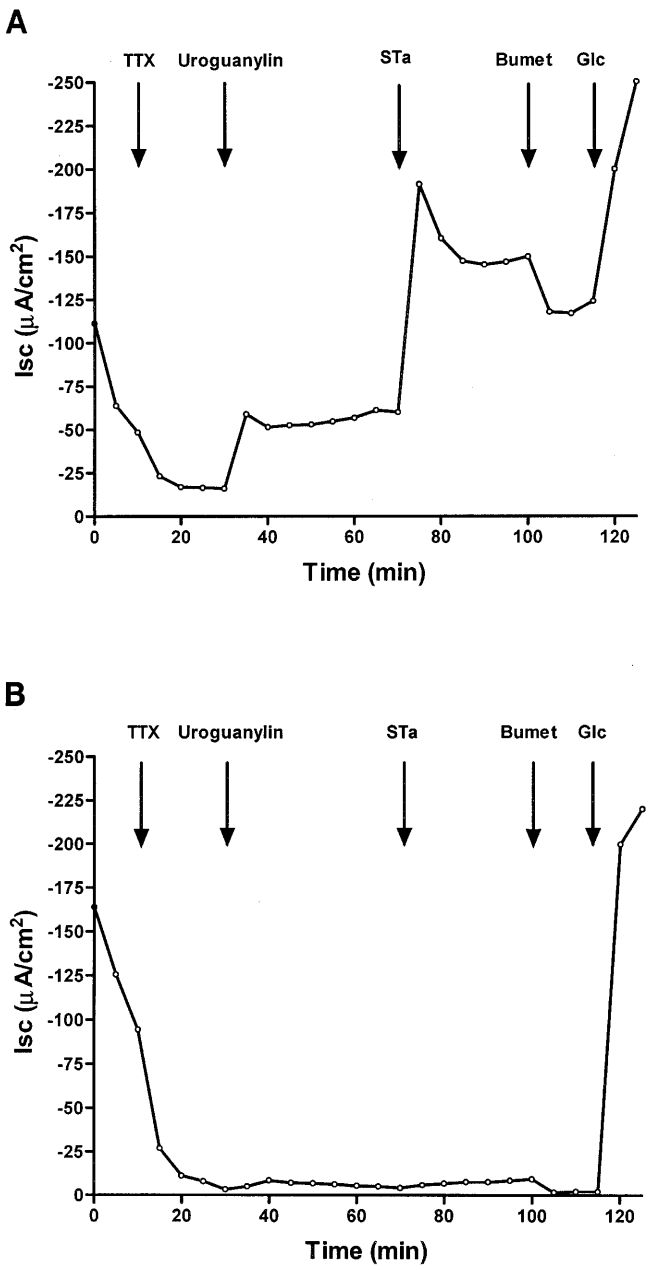

Fig. 1. Time course of short-circuit current (I_{sc}) response to sequential treatments in mouse intestine. Data are representative of 11 separate experiments with proximal duodenum bathed in standard Krebs-Ringer-bicarbonate (KRB). *A*: uroguanylin (1.0 μM), *Escherichia coli* heat-stable enterotoxin (STa13; 1.0 μM), and glucose (Glc, 10 mM) were applied to the luminal bath. *B*: uroguanylin (1.0 μM) and STa (1.0 μM) were added to serosal bath. TTX (0.1 μM) and bumetanide (Bumet; 0.1 mM) were added to serosal bath.

bioactivity in the native intestine, the pH of the luminal bath was reduced to 5.0–5.5 for 20 min before the tissue was treated with the peptide agonists (pH adjustment period). The proximal duodenum was chosen because this segment elicited pronounced increases in uroguanylin-induced I_{sc} (Fig. 2) and because this part of the small intestine has an acidic intraluminal environment during digestion (1). The intraluminal pH reduction caused a rapid and reproducible increase in the I_{sc} of 13.4 ± 2.7 μA/cm², reaching a new steady-state I_{sc} baseline in about 5 min (Fig. 3*A*, pH adjustment period). A recent study suggests that the acid-induced current may represent stimulation of electrogenic, CFTR-dependent HCO_3^- secretion in the murine duodenum (30). Subsequent uroguanylin treatment at the acidic pH produced an approximately twofold greater ($P < 0.05$) increase in I_{sc} than was observed at pH 7.4 (Fig. 3, *A* and *B*). Again, the increased I_{sc} elicited by uroguanylin was only partially inhibited by bumetanide treatment: 18.7 ± 5.7% at pH 7.4 and 27.0 ± 8.0% at pH 5.0–5.5 (Fig. 3*B*). At both pH conditions, uroguanylin treatment slightly increased G_t, but the changes were not statistically different from each other: 2.0 ± 0.4 mS/cm² at pH 7.4 and 3.1 ± 0.3 mS/cm² at acidic pH. The effect of luminal acidity on uroguanylin bioactivity in jejunal tissue was also examined. The reduction of intraluminal pH to 5.0–5.5 again increased basal I_{sc} (19.6 ± 4.8 μA/cm²), and subsequent treatment with 1.0 μM uroguanylin at acidic pH produced a significantly larger increase in I_{sc} than was observed at pH 7.4 (66 ± 4.2 vs. 44.6 ± 5.8 μA/cm², $P < 0.05$, $n = 4$). In a dose-response study, uroguanylin was more active ($P < 0.05$) in acidic luminal conditions than at pH 7.4 within the tested range of concentrations (Fig. 4). It was not possible to test higher concentrations of uroguanylin because the supply of the peptide was inadequate for the experiment.

Effect of luminal acidity on the actions of 8-BrcGMP and 8-BrcAMP. To test whether the effect of luminal acidity on uroguanylin action resulted from an effect of low extracellular pH on the bioelectric properties or intracellular signaling pathways of the epithelial cells, the I_{sc} responses elicited by membrane-permeable cyclic nucleotides, 8-BrcGMP and 8-BrcAMP, were examined at acidic and physiological pH. In the proximal

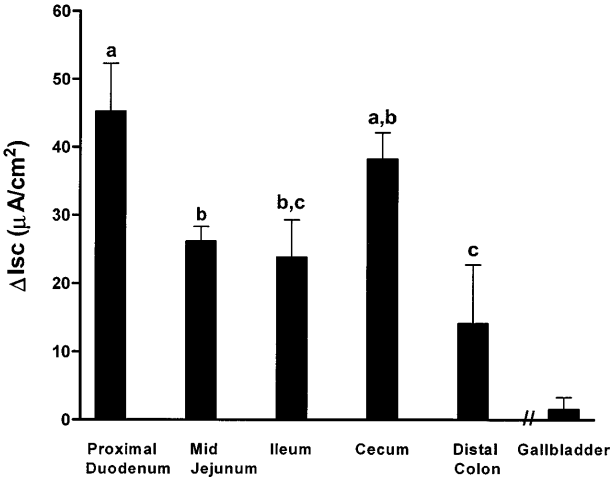

Fig. 2. Segmental responses to luminal uroguanylin in mouse intestinal preparations. All tissues were bathed with standard KRB solution. ΔI_{sc} was calculated as baseline I_{sc} minus maximal I_{sc} response to uroguanylin. Large intestinal epithelia (cecum and distal colon) were pretreated with amiloride (0.1 mM, luminal bath) 20 min before uroguanylin addition. Values are means ± SE obtained from proximal duodenum ($n = 11$), midjejunum ($n = 9$), ileum ($n = 9$), cecum ($n = 12$), distal colon ($n = 5$), and gallbladder ($n = 4$). Means without a letter in common are significantly different; one-way ANOVA protected least-significant difference test, $P < 0.05$.

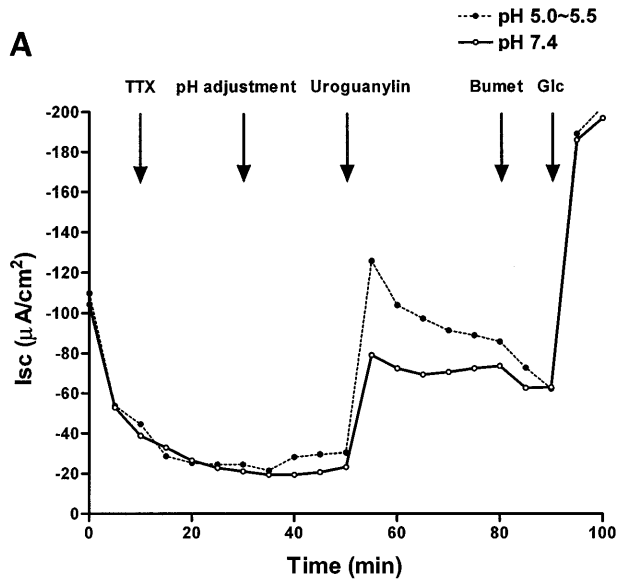

Fig. 3. Effect of pH on I_{sc} response to uroguanylin in mouse proximal duodenum. *A*: representative time course of I_{sc} response to agents in proximal duodenum superfused with Ringer solution at either pH 5.0~5.5 or pH 7.4 in luminal bath. Luminal pH was reduced to pH 5.0–5.5 by addition of 1.0 N HCl (pH adjustment), and serosal pH was maintained at 7.4. TTX (0.1 μM), uroguanylin (1.0 μM), and glucose (10 mM) were added to luminal bath, and bumetanide (0.1 mM) was added to serosal bath. *B*: cumulative data showing maximal change in I_{sc} (ΔI_{sc}) from baseline during uroguanylin treatment and after sequential addition of bumetanide (+Bumet). Results are means ± SE from intact proximal duodena of 8 (pH 7.4 group) and 9 (acid-treated group) different mice. *Significantly different from uroguanylin treatment (paired *t*-test, $P < 0.05$). †Significantly different from pH 7.4 group (unpaired *t*-test, $P < 0.05$).

duodenum, membrane-permeable 8-BrcGMP (20 μM) stimulated the I_{sc} more than did an equimolar concentration of 8-BrcAMP ($P < 0.001$) (Fig. 5). However, the I_{sc} response elicited by 8-BrcGMP at pH 7.4 was similar to that observed under acidic luminal conditions. In contrast, 8-BrcAMP (20 μM) was significantly less effective under acidic conditions than at pH 7.4 ($P < 0.05$). The increased I_{sc} elicited by either 8-BrcGMP or

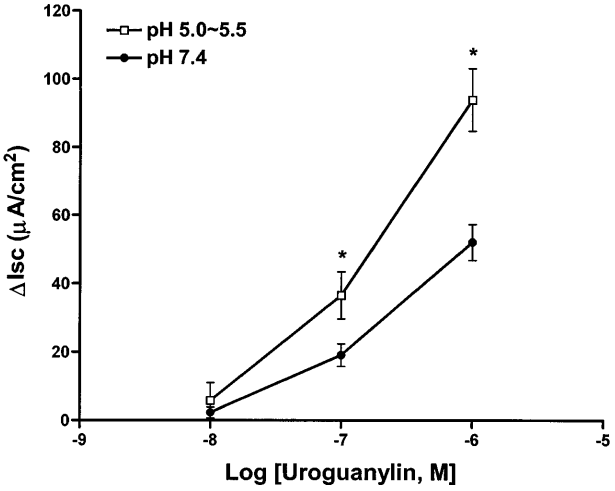

Fig. 4. Effect of luminal bath pH on noncumulative concentration-I_{sc} response curve for uroguanylin in intact mouse proximal duodenum. Luminal bath pH was reduced to 5.0–5.5 by addition of 1.0 N HCl, and basolateral pH was maintained at pH 7.4. ΔI_{sc} was calculated as baseline I_{sc} minus maximal I_{sc} response to uroguanylin. Values are means ± SE obtained from 4–9 different mice. *Significantly different from pH 7.4 group (unpaired *t*-test, $P < 0.01$).

8-BrcAMP was significantly inhibited ($P < 0.05$) by bumetanide (0.1 mM) treatment: 59.3 ± 1.8% at pH 7.4 and 65.7 ± 3.4% at pH 5.0–5.5, or 61.5 ± 5.9% at pH 7.4 and 90.8 ± 4.2% at pH 5.0–5.5, respectively.

Effect of luminal acidity on guanylin and STa actions. To investigate whether the pH dependence was specific for uroguanylin action, we examined the effects of acidic pH on the secretagogue actions of guanylin and STa (Fig. 6). Whereas uroguanylin is more effective in stimulating the I_{sc} under acidic luminal conditions

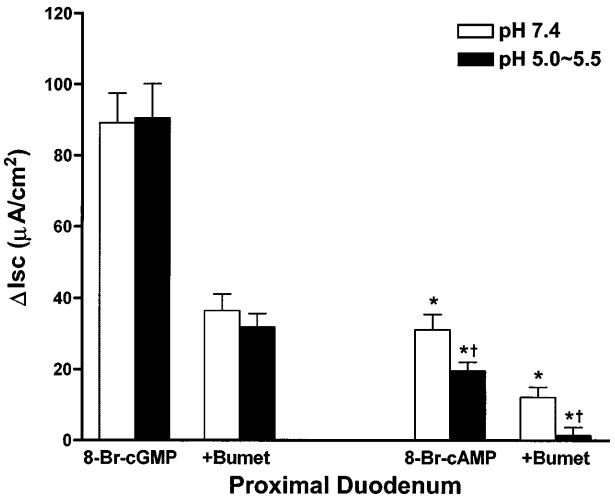

Fig. 5. Effect of luminal bath pH on I_{sc} response to membrane-permeable cyclic nucleotides in mouse proximal duodenum. 8-BrcGMP (20 μM) or 8-BrcAMP (20 μM) was added to both luminal and serosal baths 20 min after pH adjustment. Bumetanide (0.1 mM) was added to serosal bath 30 min later. ΔI_{sc} was calculated as baseline I_{sc} minus maximal I_{sc} response during cyclic nucleotide treatment and after subsequent treatment with bumetanide. Data are means ± SE; proximal duodena were obtained from 4–6 different mice in each cyclic nucleotide treatment group. *Significantly different from 8-BrcGMP-treated group (unpaired *t*-test; $P < 0.001$). †Significantly different from pH 7.4 (unpaired *t*-test; $P < 0.05$).

DOCKET ALARM

Explore Litigation Insights

Docket Alarm provides insights to develop a more informed litigation strategy and the peace of mind of knowing you're on top of things.

Real-Time Litigation Alerts

Keep your litigation team up-to-date with **real-time alerts** and advanced team management tools built for the enterprise, all while greatly reducing PACER spend.

Our comprehensive service means we can handle Federal, State, and Administrative courts across the country.

Advanced Docket Research

With over 230 million records, Docket Alarm's cloud-native docket research platform finds what other services can't. Coverage includes Federal, State, plus PTAB, TTAB, ITC and NLRB decisions, all in one place.

Identify arguments that have been successful in the past with full text, pinpoint searching. Link to case law cited within any court document via Fastcase.

Analytics At Your Fingertips

Learn what happened the last time a particular judge, opposing counsel or company faced cases similar to yours.

Advanced out-of-the-box PTAB and TTAB analytics are always at your fingertips.

API

Docket Alarm offers a powerful API (application programming interface) to developers that want to integrate case filings into their apps.

LAW FIRMS
Build custom dashboards for your attorneys and clients with live data direct from the court.

Automate many repetitive legal tasks like conflict checks, document management, and marketing.

FINANCIAL INSTITUTIONS
Litigation and bankruptcy checks for companies and debtors.

E-DISCOVERY AND LEGAL VENDORS
Sync your system to PACER to automate legal marketing.